Materials Science

Two- and Three-Dimensional Mesoporous Iron Oxides with Microporous Walls**

*Feng Jiao and Peter G. Bruce**

There is intense interest in preparing mesoporous transition-metal oxides—in part because of their potential applications, including for catalysis, electron transfer, energy conversion and storage, and as magnetic materials.[1,2] Several mesoporous transition-metal oxides have been prepared, such as TiO_2, ZrO_2, Nb_2O_5, WO_3, and MnO_x,[3,4] however, mesoporous iron oxides are of particular interest. Reversible intercalation of Li can occur for nanoparticlate Fe_2O_3, but it is much more difficult to carry out such intercalation with Fe_2O_3 of normal particle size. Similar behavior may be possible with mesoporous iron oxides since the walls are of nanodimensions. The limited dimensions of the walls will also alter the magnetic behavior from that of bulk Fe_2O_3. Although disordered iron oxides with high surface areas (ca. 270 $m^2 g^{-1}$) have been prepared, to the best of our knowledge no ordered mesoporous iron oxides have been synthesized directly.[5] Herein, we report the synthesis of ordered mesoporous Fe_2O_3 with controllable pore structures. Ordered two-dimensional (2D) hexagonal mesoporous iron oxide (2DMIO) with *P6mm* symmetry and three-dimensional (3D) cubic mesoporous iron oxide (3DMIO) with *Fm3m* symmetry have been prepared by using decylamine as the template and Fe^{III} ethoxide as the precursor. Different aging conditions were used for 2DMIO and 3DMIO, and in both cases, the walls exhibit a microporous structure.

We first confirmed successful removal of the template from 2DMIO and 3DMIO by elemental analysis. As-prepared 2DMIO contained C 44.0%, H 9.69%, and N 4.82% by weight, while the 2DMIO after ethanol extraction contained C 6.48%, H 2.17%, and N 0.28%. As-prepared 3DMIO contained C 37.9%, H 8.80%, and N 4.14%, while the values for 3DMIO after ethanol extraction were C 7.08%, H 1.71%, and N 0.35%. Based on the elemental analysis for nitrogen, about 94% and 92% of the template had been removed from 2DMIO and 3DMIO, respectively. Slightly high C and H contents were observed after removal of the template, which may correspond to a small amount of ethanol remaining in the pores (< 7% by weight in both cases).

A transmission electron microscopy (TEM) image of ordered 2DMIO was recorded along the (001) direction (Figure 1a) and the corresponding electron diffraction pattern (Figure 1b) confirmed a hexagonal structure over a large area. Examination of a wide range of particles demonstrated that they all had similar structures. Combining these results with the TEM result recorded along the (110) direction (Figure 1c) led to the conclusion that our 2DMIO has a large-scale well-ordered 2D hexagonal array of mesopores, similar to those typically observed in 2D hexagonal mesoporous silica materials, such as MCM-41 and SBA-15.[6] The TEM results recorded along the (110) direction confirmed that the mesoporosity exists throughout the particles, not just near surface regions. An average pore size of 70 Å and wall thickness of 40 Å, with a cell parameter a_0 of 110 Å, were estimated from the high-resolution transmission electron microscopy (HRTEM) image recorded along the (001) direction of as-prepared 2DMIO (Figure 1d). The low-angle powder X-ray diffraction (PXRD) pattern (Figure 2a) of as-prepared 2DMIO exhibits a diffraction peak at $2\theta = 1.14°$, which translates to a d spacing of 97.6 Å ($Fe_{K\alpha_1}$, $\lambda = 1.936$ Å). The peak may be indexed as the (100) reflection, based on the hexagonal space group *P6mm* identified by TEM/electron

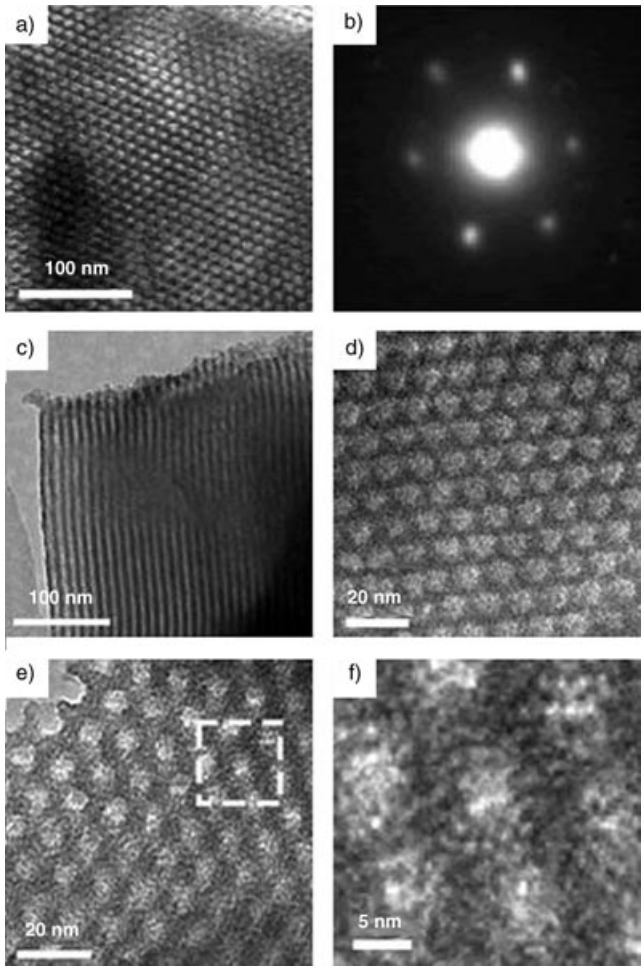

Figure 1. a) TEM image of as-prepared 2DMIO recorded along the (001) direction, b) the corresponding electron diffraction pattern, c) TEM image recorded along the (110) direction. The HRTEM images recorded along the (001) direction of d) as-prepared 2DMIO and e) after ethanol extraction. f) Enlarged HRTEM image of a selected area of (e).

[*] F. Jiao, Prof. Dr. P. G. Bruce
School of Chemistry
University of St. Andrews
The Purdie Building, North Haugh, St Andrews KY16 9ST (UK)
Fax: (+44) 1334-463-808
E-mail: p.g.bruce@st-and.ac.uk

[**] P.G.B. is indebted to the EPSRC, the Royal Society, and the EU for financial support. The authors are grateful to J.-C. Jumas, Montpellier, for carrying out the Moessbauer measurements.

  DOI: 10.1002/ange.200460826

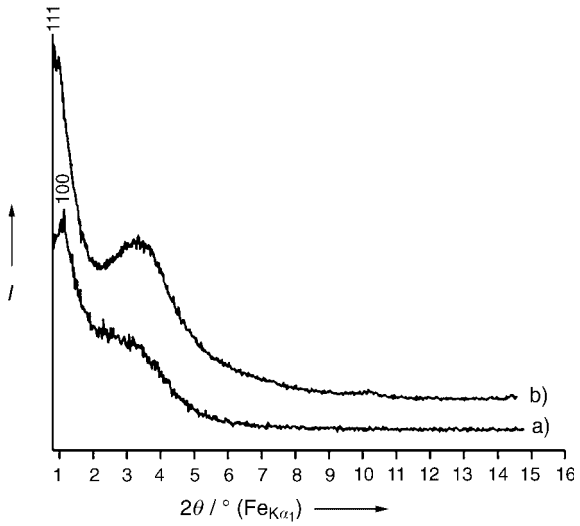

Figure 2. Low-angle PXRD patterns: a) as-prepared 2DMIO; b) as-prepared 3DMIO.

diffraction analysis. The (100) reflection corresponds to a unit cell parameter a_0 of 113 Å, which is in good agreement with the TEM data. From the well-ordered hexagonal arrangement of mesopores revealed in Figure 1 a–c, peaks might also be expected in the PXRD pattern at $2\theta = 1.97$ and 2.29°, which corresponds to d spacings of 56.4 and 48.4 Å for the (110) and (200) reflections, respectively. These peaks are not evident. This appears to result, at least in part, from the existence of a broad peak in the range of 2θ from 2.2 to 4°, which corresponds to d spacings between 25 and 45 Å. Such a broad peak is consistent with disordered microporous regions within the walls as observed by HRTEM (Figure 1 f) and discussed later. After removing the template by ethanol extraction, the HRTEM image of 2DMIO (Figure 1 e) shows a smaller average pore size of 54 Å and a wall thickness of 51 Å; the reduced pore diameter is a consequence of shrinkage accompanying removal of the decylamine. Such a pore size is larger than those previously reported for mesoporous transition-metal oxides templated by alkyl amines of comparable size, such as TiO_2 and Nb_2O_5,[1,4,7] which indicates the formation mechanism may be different in the present case. Samples of 2DMIO were calcined at various temperatures to investigate the thermal stability. TEM analysis confirmed that the mesostructure was thermally stable up to 250 °C. Moessbauer measurements indicate that the Fe oxidation state is +3 (high spin) and that the iron is in an octahedral environment of oxygen atoms. More details concerning the Moessbauer studies will be published subsequently, along with magnetic measurements; however, the Moessbauer data suggest superparamagnetic behavior consistent with the small (approximately 51 Å) dimensions of the walls.

A detailed examination of the HRTEM image (Figure 1 f) for as-prepared 2DMIO shows a large quantity of disordered micropores within the walls and with pore sizes of around 10 Å. This observation suggests that the mechanism for the formation of 2DMIO mesopores may involve self-assembly of microporous structures. Further extensive studies will be required to understand the exact nature of the formation mechanism for this micro-/mesoporous solid, including the role of the template and self-assembly of microporous structures into the micro-/mesoporous solid; this is beyond the scope of the present study. The microporosity of 2DMIO is further confirmed by nitrogen adsorption/desorption analysis. The N_2 adsorption/desorption isotherms (Figure 3 a) for

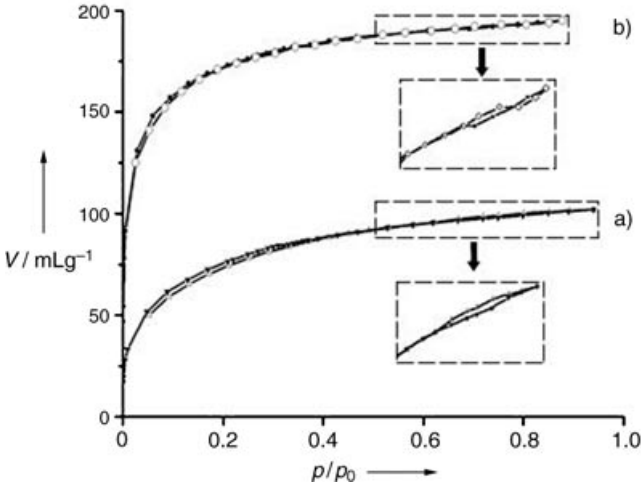

Figure 3. Nitrogen adsorption/desorption isotherms: a) 2DMIO and b) 3DMIO after ethanol extraction. The inset shows an enlarged region of the curves between relative pressures of 0.6 and 0.8.

2DMIO after removal of the template show predominantly a type I curve, thus indicating that the dominant surface area is in fact the micropores. There is a small step at a relative pressure of 0.7–0.8, which corresponds to mesoporous adsorption in 2DMIO. The identification of microporosity in the walls of mesoporous materials has only occasionally been observed before, particularly in SBA-15, MAS-7, and MTS-9.[8] There is an important and unique difference between SBA-15, MAS-7, and MTS-9 and our materials: The ratio of micropores to mesopores is much higher in the transition-metal oxides, as is evident from the small mesopore adsorption at relative pressures of 0.7 and 0.8. As the TEM image clearly indicates significant mesoporosity, we propose that the surfaces of the mesoporous walls may themselves be highly microporous so that N_2 "sees" a mainly microporous material during adsorption. The Brunauer–Emmett–Teller (BET) surface area of 2DMIO is 340 $m^2 g^{-1}$.

Our approach can also be used to prepare three-dimensional mesoporous iron oxides by adjusting the aging temperature. Ordered 3D cubic mesoporous iron oxide (3DMIO) with $Fm3m$ symmetry is obtained when the Fe^{III} ethoxide/decylamine mixture is further aged at 150 °C. TEM images recorded from different directions (Figure 4 a–c) confirmed the large area of ordered cubic F$m3m$ mesoporous iron oxides, and Moessbauer measurements confirmed that the oxidation state is +3. The low-angle PXRD spectra (Figure 2 b) show a main diffraction peak at $2\theta = 1.06°$, which corresponds to a d spacing of 104.6 Å. The unit cell parameter a_0 calculated from the PXRD pattern is 182 Å, which is in reasonable agreement with the value of 192 Å determined

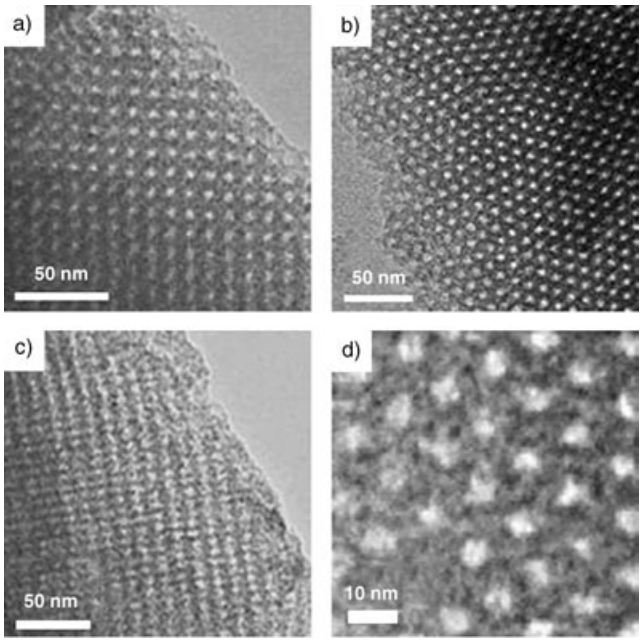

Figure 4. TEM images of 3DMIO recorded along the: a) (100) direction; b) (110) direction; c) (211) direction. d) Enlarged region of (b).

from the TEM analysis. Microporosity similar to that observed in 2DMIO is seen in 3DMIO by HRTEM (Figure 4d) and in the N_2 adsorption/desorption analysis (Figure 3b). The BET surface area calculated from the desorption isotherm is approximately 610 $m^2 g^{-1}$, which is about twice that for 2DMIO, perhaps because of the higher accessible pore surface in the three-dimensional structure.

The simultaneous presence of micro- and mesoporous structures is not common. This is the first time alkyl amine templates have been used as bifunctional surfactants which can template micro- as well as mesostructures.

Experimental Section

The synthesis procedure was adapted from that employed for Nb_2O_5.[4] In a typical synthesis of 2D hexagonal ordered mesoporous Fe_2O_3, Fe^{III} ethoxide (0.573 g, 3 mmol; 99%, ABCR) was dissolved in ethanol (35 mL), with stirring for 5 minutes, followed by addition of decylamine (0.472 g, 3 mmol; 95%, Aldrich). After stirring the mixture at 40°C for 2 h, it was maintained at 40°C for 24 h, and further aged at 80°C for 6 h. In the case of 3DMIO, additional aging at 150°C was carried out. The products were then filtered and washed with ethanol. The template may be removed by extraction with excess ethanol. As-prepared material (0.1 g) was added to ethanol (100 mL) with stirring at RT for 30 min, followed by filtration and drying at 70°C under vacuum for 1 h. The materials before and after template removal were characterized by elemental analysis (Carlo Erba CHNS analyzer), TEM (Jeol JEM-2011), PXRD (Stoe STADI/P diffractometer operating in transmission mode with $Fe_{K\alpha_1}$ radiation, $\lambda = 1.936$ Å), N_2 adsorption (Hiden IGA porosimeter), and Moessbauer spectroscopy (^{57}Fe Moessbauer spectra, collected at RT on a EG&G constant accelerator spectrometer in transmission mode).

Received: May 28, 2004
Published Online: August 20, 2004

Keywords: materials science · mesoporous materials · microporous materials · transition metals

[1] D. M. Antonelli, J. Y. Ying, *Angew. Chem.* **1995**, *107*, 2202; *Angew. Chem. Int. Ed. Engl.* **1995**, *34*, 2014.
[2] a) F. Schüth, *Chem. Mater.* **2001**, *13*, 3184; b) P. Yang, T. Deng, D. Zhao, P. Feng, D. Pine, B. F. Chmelka, G. M. Whitesides, G. D. Stucky, *Science* **1998**, *282*, 2244; c) X. He, D. Antonelli, *Angew. Chem.* **2002**, *114*, 222; *Angew. Chem. Int. Ed.* **2002**, *41*, 214; d) P. Behrens, *Angew. Chem.* **1996**, *108*, 561; *Angew. Chem. Int. Ed. Engl.* **1996**, *35*, 515; e) Q. S. Huo, D. I. Margolese, U. Ciesla, D. G. Demuth, P. Y. Feng, T. E. Gier, P. Sieger, A. Firouzi, B. F. Chmelka, F. Schuth, G. D. Stucky, *Chem. Mater.* **1994**, *6*, 1176.
[3] a) P. Yang, D. Zhao, D. I. Margolese, B. F. Chmelka, G. D. Stucky, *Nature* **1998**, *396*, 152; b) Z. Tian, W. Tong, J. Wang, N. Duan, V. V. Krishnan, S. L. Suib, *Science* **1997**, *276*, 926; c) B. Tian, H. Yang, X. Liu, S. Xie, C. Yu, J. Fan, B. Tu, D. Zhao, *Chem. Commun.* **2002**, 1824; d) E. L. Crepaldi, G. J. de A. A. Soler-Illia, D. Grosso, F. Cagnol, F. Ribot, C. Sanchez, *J. Am. Chem. Soc.* **2003**, *125*, 9770; e) N. Ulagappan, C. N. R. Rao, *Chem. Commun.* **1996**, 1685; f) X. Xu, B. Tian, J. Kong, S. Zhang, B. Liu, D. Zhao, *Adv. Mater.* **2003**, *15*, 1932.
[4] D. M. Antonelli, A. Nakahira, J. Y. Ying, *Inorg. Chem.* **1996**, *35*, 3126.
[5] a) D. N. Srivastava, N. Perkas, A. Gedanken, I. Felner, *J. Phys. Chem. B* **2002**, *106*, 1878; b) A. S. Malik, M. J. Duncan, P. G. Bruce, *J. Mater. Chem.* **2003**, *13*, 2123.
[6] a) C. T. Kresge, M. E. Leonowicz, W. J. Roth, J. C. Vartulli, J. S. Beck, *Nature* **1992**, *357*, 710; b) D. Y. Zhao, J. L. Feng, Q. S. Huo, N. Melosh, G. H. Fredrickson, B. F. Chmelka, G. D. Stucky, *Science* **1998**, *279*, 548.
[7] T. Sun, J. Y. Ying, *Nature* **1997**, *389*, 704.
[8] a) M. Kruk, M. Jarnoiec, C. H. Ko, R. Ryoo, *Chem. Mater.* **2000**, *12*, 1961; b) P. I. Ravikovitch, A. V. Neimark, *J. Phys. Chem. B* **2001**, *105*, 6817; c) J. Liu, X. Zhang, Y. Han, F. S. Xiao, *Chem. Mater.* **2002**, *14*, 2536.
[9] Note after publication of this manuscript online on August 20, 2004 in the Early View mode: The TEM data shown in Figures 1 and 4 indicate an ordered mesostructure prior to template removal and suggest the presence of mesopores in the material after template removal, yet the N_2 isotherms do not show the typical behavior expected for large mesopores of around 5 nm. It

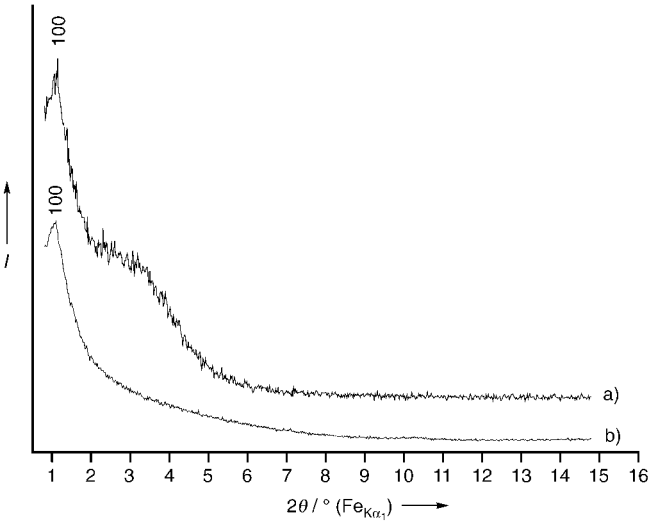

Figure 5. Low-angle PXRD patterns: a) as-prepared 2DMIO and b) 2DMIO after removal of the template.

should, however, be noted that pore dimensions are not well-determined by TEM. The N_2 isotherms are consistent with smaller mesopores (M. Kruk and M. Jaroniec, *Chem. Mater.* **2001**, *13*, 3169), as observed in mesoporous TiO_2 (D. M. Antonelli, *Micropor. Mesopor. Mater.* **1999**, *30*, 315), and the presence of microporosity; they also indicate that the pores are distributed in size. Further work is required to rationalize the isotherms and TEM data in detail. One possible explanation is that the pores shrink unevenly on removal of the template, thus leading to distortion of the pores and rough walls; some material may even detach from the walls and locate within the pores. As a result the pores cannot be described as regular cylinders and exhibit a smaller effective diameter than suggested by TEM. The TEM data after template removal (for example, Figure 1e) are consistent with pores that are more distorted than prior to removal of the template. An X-ray diffraction pattern after removal of the template shows one low-angle peak (see Figure 5) indicating that the pore order is not sufficient to generate higher angle peaks.

